

Assignment of the Vibrations of Unsubstituted BODIPY and Aza-BODIPY

Alexander E. Pogonin,[@] Darya A. Postnikova, Artyom Y. Shagurin, Danila V. Belov, Sergey D. Usoltsev, and Yuriy S. Marfin

Ivanovo State University of Chemistry and Technology, 153000 Ivanovo, Russian Federation

[@]Corresponding author E-mail: pogonin@isuct.ru

According to quantum chemical calculations generic BODIPY and aza-BODIPY both have planar structure. Assignment of vibrational modes of BODIPY and aza-BODIPY was carried out via potential energy distribution analysis among internal coordinates. Despite obvious similarity of the structure and normal modes of the molecules, there are perceptible differences in simulated IR spectra, which were noted. Analysis of the simulated spectra and the experimental data available in literature allowed us to conclude that most of the bands observed in the IR spectra correspond to separate vibrational transitions. The complicated composition of most of the vibrational modes should be noted. The obtained data will also be useful in studies of substituted BODIPY and aza-BODIPY derivatives since it provides solid foundation for systematic assignment of vibrational bands in these molecules.

Keywords: BODIPY, vibrational spectra, quantum chemical calculation, normal mode.

Интерпретация колебаний незамещенных BODIPY и aza-BODIPY

А. Е. Погонин,[@] Д. А. Постникова, А. Ю. Шагурин, Д. В. Белов, С. Д. Усольцев, Ю. С. Марфин

Ивановский государственный химико-технологический университет, 153000 Иваново, Российская Федерация

[@]E-mail: pogonin@isuct.ru

Согласно результатам квантово-химических расчетов молекулы BODIPY и aza-BODIPY имеют плоское строение. Проведено описание колебаний молекул BODIPY и aza-BODIPY на основе анализа распределения потенциальной энергии (РПЭ) форм нормальных колебаний по естественным колебательным координатам. РПЭ нормальных колебаний по внутренним координатам в рассматриваемых молекулах в большинстве случаев имеет сложный характер. Показано, что, несмотря на сходство структур и колебаний молекул BODIPY и aza-BODIPY, существуют заметные отличия теоретических ИК спектров рассматриваемых соединений. Сопоставление рассчитанных ИК спектров и имеющихся в литературе экспериментальных данных показывает, что большинство наблюдаемых полос в ИК спектре могут быть отнесены к отдельным колебательным переходам. При этом большинство колебательных мод имеет сложный характер. Данные, полученные в настоящей работе, полезны для проведения дальнейших систематических исследований колебательных спектров и колебаний в молекулах замещенных BODIPY и aza-BODIPY.

Ключевые слова: BODIPY, колебательные спектры, квантовая химия, нормальные колебания.

Introduction

Constant search for new compounds is an important part of the development in any scientific area. In this regard, synthesis, experimental studies and quantum chemical (QC) calculations are closely intertwined. Simulations can greatly accelerate the identification, characterization and optimization of materials.^[1] Matching experimental measurements with theoretical predictions provides good insight into relations between molecular structure and physico-chemical properties, providing a solid ground for further investigations. Currently, QC calculations are often used in dyes chemical physics to simulate electronic absorption and fluorescence spectra. Derivatives of 4,4'-difluoro-4-bora-3a,4a-diaza-s-indacene (BODIPY) and 4,4'-difluoro-4-bora-3a,4a,8-triaza-s-indacene (aza-BODIPY) have gained increasing interest in two recent decades.^[2] This is caused by the fact, that these substances display very promising optical properties: high molar extinction coefficients, fluorescence quantum yields and narrow electronic absorption and emission bands. Alteration of properties of BODIPY and aza-BODIPY is carried out via corresponding substitution pattern modification leading to ultraviolet-visible (UV-Vis) and luminescence bands shift as well as achievement of their sensitive response towards specific solvent parameters.^[3–7] Good prediction of these properties is of a paramount importance in the field of dye chemistry.

As for now, vibration spectroscopy is used in BODIPY studies mainly as one of the ways to prove the identity of compounds. However, infrared (IR) and Raman spectroscopies are versatile techniques for studying the intrinsic properties of various compounds. In the literature, there is a clear lack of data on detailed assignment of the vibrational bands for BODIPYs, while many studies focused on the description of vibrations of various larger molecules, *e.g.* porphyrins^[8,9] and phthalocyanines.^[10,11] Among a few studies dedicated to BODIPYs vibrations, we should mention the work,^[12] in which the vibrational frequencies experimentally extracted from two-dimensional electronic spectra (2DES) were compared to the DFT calculated Raman spectra. Differences between calculated Raman active modes and experimental frequencies are explained by the fact that

the QC calculations were performed on the ground state and do not include changes that may occur in the excited electronic state.^[12] In the case of literature data on BODIPYs, most often, attention is paid to individual vibration bands only. In order to get a consistent description of complex BODIPY derivatives and to systematize information about the effect of substitution on spectroscopic properties, we found it important to study generic BODIPY and aza-BODIPY structures. The lack of detailed information on vibrational spectra can be explained by the fact that the generic BODIPY structure had not been synthesized until 2009.^[13–15]

For big cyclic compounds it is not appropriate to simply assign any experimental peak to the vibration of one certain bond.^[16] Sometimes the entire molecule should be considered as a whole for the proper interpretation. QC calculations help assign the bands in experimental vibrational spectra. To interpret a model of vibrational spectra a visualization of the nuclei movement and potential energy distribution (PED) analysis were used.^[17]

Calculation Details

QC calculations were performed using the Gaussian 03 program^[18] in the framework of density functional theory (DFT) method. Optimized geometries and all of the harmonic vibrational frequencies were obtained using B3LYP functional with cc-pVTZ basis set^[19] for all atoms. The basis set was taken from Basis Set Exchange software.^[20–22] The assignment of vibrational modes was carried out by the PED analysis among internal coordinates using the VibModule program.^[23] Visualization of vibrations is realized by the ChemCraft software.^[24]

Results and Discussion

Molecular Structure

The QC calculations predict a C_{2v} equilibrium structures for both BODIPY and aza-BODIPY with planar dipyrromethene moiety. This is in consistent with the information available in the literature.^[25–27] Upon the replacement of C_8-H group by an N_8 atom (BODIPY→aza-BODIPY),

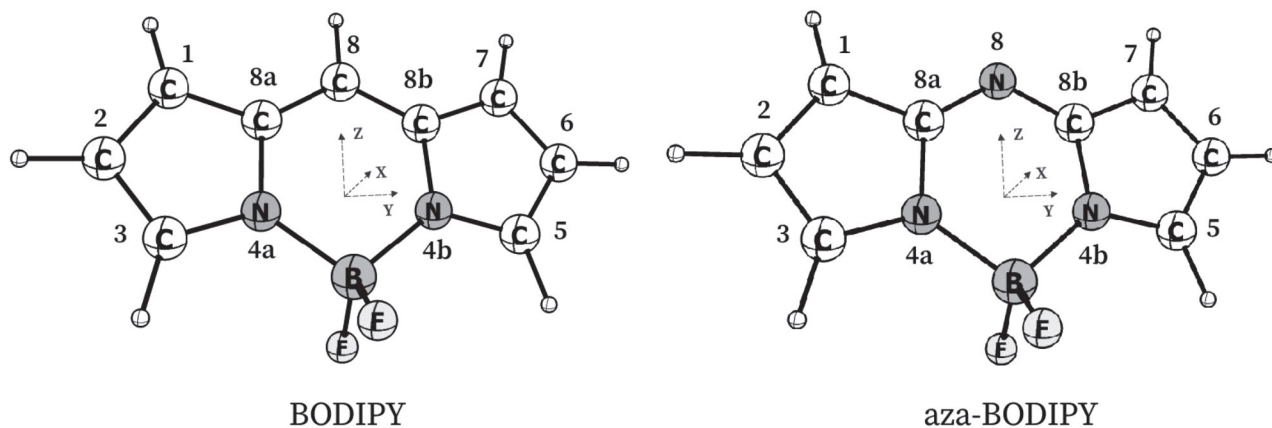


Figure 1. Atom numbering/labeling scheme for BODIPY and aza-BODIPY.

Table 1. Selected structural parameters of BODIPY from B3LYP calculations and from X-ray data^[13–15] in comparison with structural parameters of aza-BODIPY obtained by B3LYP calculations.

| Parameters ^a | BODIPY X-ray ^[13] | BODIPY X-ray ^[14] | BODIPY X-ray ^[15] | BODIPY B3LYP | aza-BODIPY B3LYP |
|---|---------------------------------|---------------------------------|---------------------------------|-----------------|---------------------|
| N _{4a} -C _{8a} | 1.390 ^b | 1.381 ^b | 1.400 ^b | 1.390 | 1.398 |
| C _{8a} -X ₈ | 1.384 ^b | 1.376 ^b | 1.394 ^b | 1.386 | 1.318 |
| C ₁ -C _{8a} | 1.409 ^b | 1.386 ^b | 1.418 ^b | 1.415 | 1.422 |
| N _{4a} -C ₃ | 1.339 ^b | 1.337 ^b | 1.349 ^b | 1.335 | 1.332 |
| N-B | 1.548 ^b | 1.549 ^b | 1.559 ^b | 1.573 | 1.572 |
| C ₁ -C ₂ | 1.385 ^b | 1.372 ^b | 1.375 ^b | 1.383 | 1.377 |
| C ₂ -C ₃ | 1.398 ^b | 1.391 ^b | 1.404 ^b | 1.408 | 1.414 |
| B-F | 1.392 ^b | 1.392 ^b | 1.396 ^b | 1.382 | 1.380 |
| N _{4a} -B-N _{4b} | 106.5 | 106.6 | 106.9 | 105.5 | 103.5 |
| C _{8a} -X ₈ -C _{8b} | 121.7 | 123.3 | 122.3 | 122.0 | 119.6 |
| F-B-F | 108.6 | 108.6 | 109.0 | 111.3 | 111.6 |
| C ₂ -C ₃ -N _{4a} -B | 177.2 ^b | 177.2 ^b | 177.0 ^b | 180.0 | 180.0 |
| C _{8a} -N _{4a} -B-N _{4b} | 11.1 ^b | 10.6 ^b | 10.8 ^b | 0.0 | 0.0 |
| N _{4a} -C _{8a} -X ₈ -C _{8b} | 2.0 ^b | 0.7 ^b | 2.1 ^b | 0.0 | 0.0 |

^adistances in Å, angles in deg.; ^b average values for nonequivalent parameters on the same type calculated using data.^[13–15,28]

the structure of dipyrromethene moiety is changed, although the binding to the BF₂ remains almost the same (Table 1). It should be noted, that BODIPY in its crystalline state is slightly distorted:^[13–15] the boron atom lies out of the chelate cavity plane of the ligand. The authors^[13] named this distortion “saddled”. Despite these differences, the structural parameters according to X-ray and QC calculations are in good agreement (Table 1).

Vibrations and Spectra

In order to describe the vibrations, the following axes choices^[29] were used: the z-axis is the axis of symmetry, x-axis was chosen perpendicular to the molecule plane and, finally, y is orthogonal to both (Figure 1). The BODIPY molecule belongs to the C_{2v} point group and has 57 vibrational modes: $\Gamma_{\text{vib}} = 20a_1 + 8a_2 + 11b_1 + 18b_2$. In aza-BODIPY there are 54 fundamental vibrations which have the following distribution in the symmetry classes belonging to the C_{2v} point group: $\Gamma_{\text{vib}} = 19a_1 + 8a_2 + 10b_1 + 17b_2$. Changes in the dipole moment along the x, y, z axes will happen to vibrations b₁, b₂, a₁, respectively, and thereby allow the vibrations to be IR active. All four symmetry species may be Raman active. Assignments of all vibration bands in the molecules are presented in Tables 2–4. The visualization of all vibrations can be found in the video file located in the supplementary materials. Majority of normal modes are extended over entire molecule. According to the PED, most of the vibrations are comprised of displacements along several internal coordinates, which complicates the frequency assignment. In the variety of complex vibrations, “simple” vibrations ω_{36} and ω_{51} should be noted: they originate from B-F stretching (> 80 %) and C₈-H₈ stretching (~100 %), respectively. Vibra-

tions ω_{52} - ω_{57} can be assigned to C-H stretching in pyrrole moieties. A significant contribution (~40–50 %) to ω_{5-8} modes is made by in-plane bending motions of a chelate. Out-of-plane modes ω_{13} and ω_{15} , ω_{16} and ω_{18} of BODIPY and aza-BODIPY correspond to asymmetric and symmetric torsional vibrations of pyrrole designated by the authors^[30] as τ_{ring} . Frequencies related to the C-H out-of-plane bending ($\omega_{19,20,23,24,27,28}$) lie in the range of 750–1000 cm⁻¹. The majority of modes in the range of 800–1600 cm⁻¹ are strongly coupled in-plane bending motions and stretching in the molecule skeleton.

Calculation results show that two regions with low intensities (0–750 cm⁻¹, 3180–3280 cm⁻¹) and one region with medium to high intensities (750–1700 cm⁻¹) could be distinguished in the obtained spectra (Figure 2–4). In the frequency range 1700–3100 cm⁻¹, fundamental vibrational transitions are absent. The simulation demonstrates that most of the medium and high intensity bands in the spectra correspond to separate vibrational modes. However, the bands 397 cm⁻¹, 597 cm⁻¹, 1162 cm⁻¹ (BODIPY), 256 cm⁻¹, 1087 cm⁻¹, 1168 cm⁻¹ (aza-BODIPY) are superpositions of bands corresponding to the separate vibrational transitions (Figures 2, 3). High-intensity bands at 1162 cm⁻¹ (BODIPY) and 1168 cm⁻¹ (aza-BODIPY) are composed of ω_{36} and ω_{37} vibrational modes (Figure 2, Table 3). Vibrational mode ω_{37} is more complicated than ω_{36} : it consists of stretching of B-N, B-F and C-C bonds, but stretching of B-F bonds contributes only to the extent of ~20 %.

The authors^[13] showed the location of the main bands in the IR spectrum of BODIPY. It should be noted that the positions of the bands in the obtained theoretical spectrum are in good agreement with the appropriate values

from the experimental spectrum.^[13] Correlation between the bands in model and experimental spectra for BODIPY is close to linear one (Figure 5). The obtained scaling coefficient (0.976, Figure 5) is in good agreement with expected value of 0.967^[31,32] for the B3LYP/cc-pVTZ level of theory.

Low frequency vibrations are interesting for the study of substituted cyclic compounds since they can explain the resulting distortions of the molecules. With the introduction of substituent groups in macrocycles (for example regarding porphyrins^[33]) steric hindrance arises that can be released at the expense of geometrical changes in the molecules with the use of low frequency vibrational modes. For BODIPY and aza-BODIPY mode ω_1 involves primarily displacement of boron atoms out of the chelate plane. Modes ω_{2-4} are described by out-of-plane skeletal distortions of “butterfly” and “propeller” type. Propeller vibration ω_3 (ω_4) can be represented as rotations of two pyrrole moieties around the line between C_{8a} (N_{4a}) atom and the center of the bond C_2-C_3 (C_1-C_2). It should be recalled that the BODIPY structure in the solid phase^[13-15] also has displacement of the boron atom from the chelate plane. Other authors^[34] also pointed out the presence of butterfly- and propeller-types distortion for BODIPY derivatives.

Differences between the Model Spectra of BODIPY and aza-BODIPY

Influence of the bridge moieties (*meso*-atoms C_8-H_8 and N_8) on the vibrational spectra of BODIPY and aza-BODIPY manifests itself due to: a) BODIPY has 3 extra vibrations ω_{29} , ω_{41} , ω_{51} , which have been attributed to H_8 dependent peaks; b) changes in PED, *e.g.* changes caused by combining the H_8 movement with other displacements in BODIPY; c) structural differences between molecules, which, along with similar PEDs for BODIPY and aza-BODIPY, lead to a shift in the vibration frequencies.

C_8-H_8 out-of-plane bending and C_8-H_8 stretching contribute to the extent of $\sim 65\%$ and $\sim 100\%$ to the ω_{29} and ω_{51} vibrations, respectively. However, ω_{41} mode is complex: the contribution of C_8-H_8 in-plane bending is only $\sim 25\%$. Only ω_{41} mode predicted at 1328 cm^{-1} possesses enough intensity in the IR spectrum to be identified as characteristic for BODIPY (Figure 2).

With the assistance of a visual representation analysis (*Supplementary Materials*), remaining vibrations modes of a BODIPY were found to closely relate to modes of aza-BODIPY (Tables 2–4). PED of appropriate normal modes of two molecules are similar both qualitatively and quantitatively: upon BODIPY→aza-BODIPY transition, quantitative differences in the contributions of the internal coordinates used in the work (Table 2–4) usually change by no more than $\sim 15\%$. However, examples of higher differences in PED should be denoted. Normal modes ω_{18} and ω_{20} are described by a sum of out-of-plane bending of C-H and carbon skeleton: whereas for aza-BODIPY the contributions $\gamma(\text{C-H})$ and $\gamma(\text{BODIPY})$ are approximately equal, it was found that for BODIPY just one of the coordinates dominates with the ratio of 70:30. The corresponding bands show an average upshift of 20 cm^{-1} with change of the *meso*-atom (Figure 2, region $730\text{--}800\text{ cm}^{-1}$). Contributions of the C_x-H_x stretching coordinates to $\omega_{52}\text{--}\omega_{57}$ also differ in the molecules (Table 4). Frequencies $\omega_{52}\text{--}\omega_{57}$ alter slightly for the considered molecules. Due to the low intensity of the corresponding bands in the region of $3220\text{--}3270\text{ cm}^{-1}$, those differences will be difficult to register in the experiment. In the case of BODIPY, the C_8-H_8 in-plane bending is coupled with other displacements (Table 4) for normal modes ω_{38} and ω_{40} . IR intensities for the mode ω_{40} increase upon BODIPY→aza-BODIPY transition (Table 3). It was denoted that for BODIPY a large input ($\sim 30\%$) to the whole vibration is contributed by C-H in-plane bending, while for aza-BODIPY the contribution of $\delta(\text{C-H})$ decreases to $\sim 10\%$ and the contribution $\nu(\text{NC})$ increases by $\sim 15\%$ as compared to BODIPY.

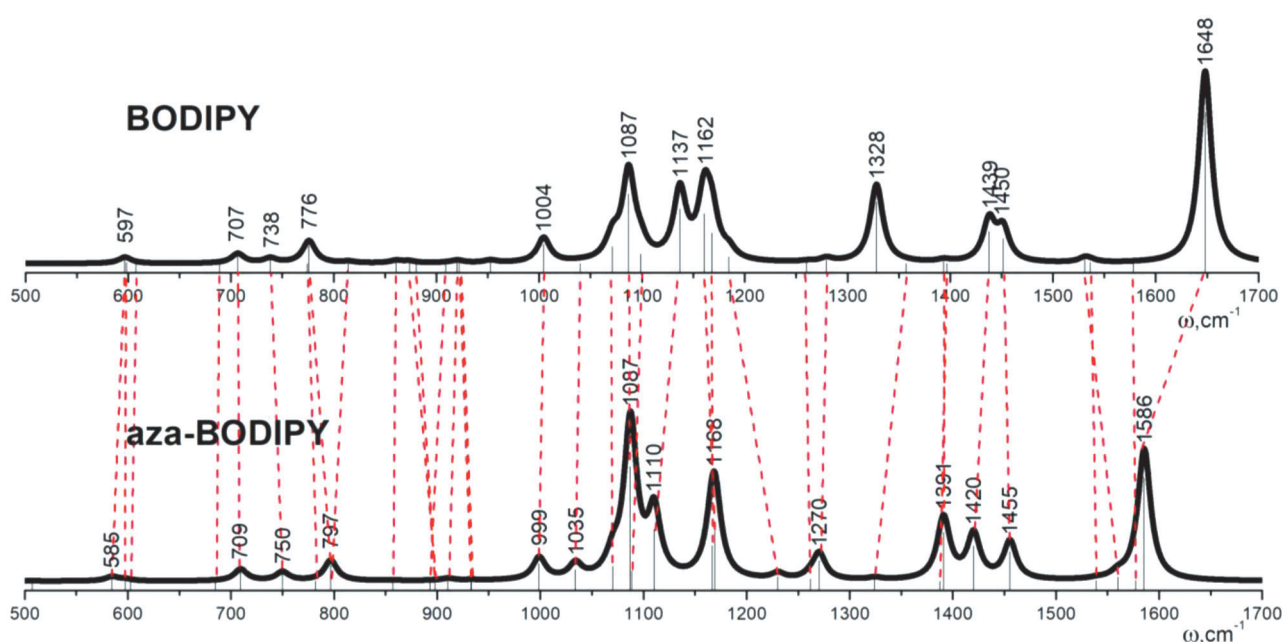


Figure 2. Simulated IR spectra for BODIPY and aza-BODIPY in the $500\text{--}1700\text{ cm}^{-1}$ range.

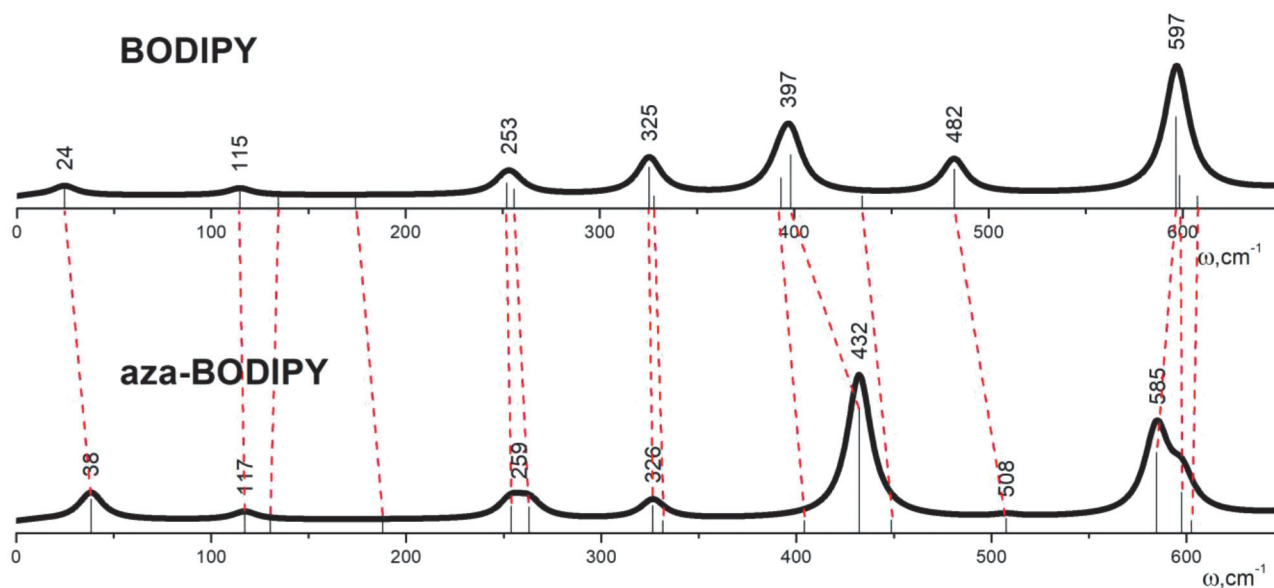


Figure 3. Simulated IR spectra for BODIPY and aza-BODIPY in the 0–650 cm^{-1} range.

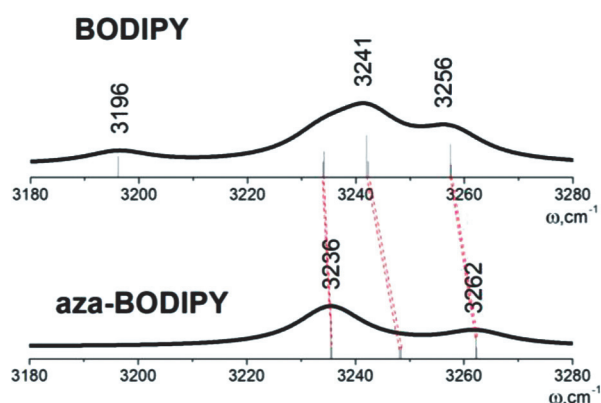


Figure 4. Simulated IR spectra for BODIPY and aza-BODIPY in the 3180–3280 cm^{-1} range.

Despite the close PED of fundamental modes of BODIPY and aza-BODIPY, nine of them are characterized by differences greater than 20 cm^{-1} ($\omega_{10,12,20,23,35,38,42,47,50}$, Tables 2–4). Upon a change from BODIPY to aza-BODIPY the maximal downshift of 63 cm^{-1} is observed for ω_{50} fundamental frequency. The mode originates from X_8-C_{8a} stretching ($\sim 60\%$) and is characterized by large IR intensity (1648 and 1586 cm^{-1} , Figure 2). In addition to the differences denoted above, spectra of the BODIPY and aza-BODIPY also differ in the area of 1100–1150 cm^{-1} and 1390–1460 cm^{-1} . The band corresponding to ω_{35} demonstrates significant contributions of C_2-C_3 and C_1-C_{8a} stretching ($\sim 50\%$). Apparently, differences in structure of pyrrole moieties due to *meso*-atom switch lead to a downshift by 27 cm^{-1} . According to the QC calculations, the IR intensity of ω_{43} vibration band increases sharply upon BODIPY \rightarrow aza-BODIPY transition, which leads to the appearance of 1391 cm^{-1} band in the simulated spectrum of aza-BODIPY. Moreover, upon BODIPY \rightarrow aza-

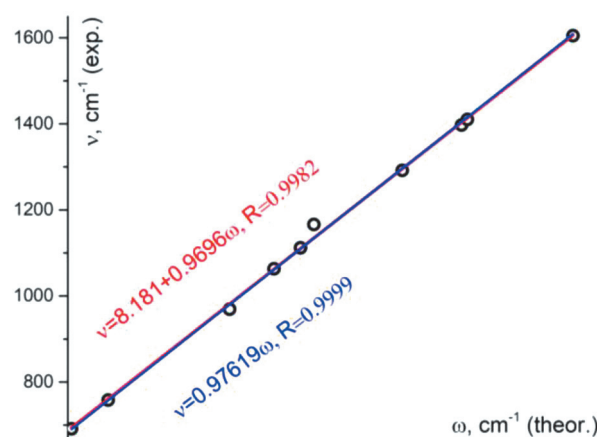


Figure 5. Correlation dependences $v = f(\omega)$: v and ω – the positions of the band maxima in the experimental^[13] and model spectra (Figure 2) for BODIPY, respectively. R – adjusted R squared.

BODIPY transition low-frequency modes ($\omega_{1,12}$) shift upwards (except for ω_3). Downshifts of frequencies are found for the C-H out-of-plane (contribution of $\gamma(\text{C-H})$ is about 70 %) modes $\omega_{19,20,23,24,27,28}$ upon BODIPY \rightarrow aza-BODIPY transition.

Conclusions

Despite the uniquely great interest shown in substituted BODIPYs and aza-BODIPYs, little attention has so far been paid to the parent molecules. This is unacceptable for the systematic study of more complex molecules and the study of the effect of substitution in these molecules. In this work we systematically designated the vibrations

Table 2. Calculated frequencies (ω_i , cm^{-1}), I-intensities ($I_{\text{IR}i}$, km mol^{-1}) and vibrational modes descriptions* for BODIPY and aza-BODIPY in the 0–650 cm^{-1} range.

| i | sym | BODIPY | | aza-BODIPY | |
|----|----------------|----------------------------|---|----------------------------|---|
| | | $\omega_i(I_{\text{IR}i})$ | Assignment* | $\omega_i(I_{\text{IR}i})$ | Assignment* |
| 1 | b ₁ | 24.5(1.8) | $\gamma(\text{B}); \text{rot}(\text{Py}; \text{N}_{4a} \cdots \text{Ct}(\text{C}_1-\text{C}_2))$ | 38.4(5.1) | $\gamma(\text{B}); \text{rot}(\text{Py}; \text{N}_{4a} \cdots \text{Ct}(\text{C}_1-\text{C}_2))$ |
| 2 | b ₁ | 114.7(1.3) | butterfly | 117.2(1.5) | butterfly |
| 3 | a ₂ | 134.6(0.0) | propeller = $\text{rot}(\text{Py}; \text{C}_{8a} \cdots \text{Ct}(\text{C}_2-\text{C}_3)); \text{rot}(\text{BF}_2)$ | 130.3(0.0) | propeller = $\text{rot}(\text{Py}; \text{C}_{8a} \cdots \text{Ct}(\text{C}_2-\text{C}_3)); \text{rot}(\text{BF}_2)$ |
| 4 | a ₂ | 174.3(0.0) | propeller = $\text{rot}(\text{Py}; \text{N}_{4a} \cdots \text{Ct}(\text{C}_1-\text{C}_2)); \text{rot}(\text{BF}_2)$ | 187.9(0.0) | Propeller = $\text{rot}(\text{Py}; \text{N}_{4a} \cdots \text{Ct}(\text{C}_1-\text{C}_2)); \text{rot}(\text{BF}_2)$ |
| 5 | b ₂ | 252(3.1) | def(BODIPY); wag(F); $\nu(\text{B}-\text{N}_{4a})$ | 253.8(3.5) | def(BODIPY); wag(F); $\nu(\text{B}-\text{N}_{4a})$ |
| 6 | a ₁ | 255.7(1.6) | def(BODIPY); $\nu(\text{B}-\text{N}_{4a})$ | 262.9(3.2) | def(BODIPY); $\nu(\text{B}-\text{N}_{4a})$ |
| 7 | a ₁ | 325.3(6.8) | def(m-ring); sci(F-B-F) | 326.4(3.6) | def(m-ring); sci(F-B-F) |
| 8 | a ₂ | 327.6(0.0) | rot(BF ₂); wav | 331.4(0.0) | rot(BF ₂); wav |
| 9 | b ₁ | 393.1(4.3) | $\gamma(\text{BODIPY}); \gamma(\text{C}_8, \text{B}, \text{C}_1, \text{C}_3);$ | 404(0.0) | $\gamma(\text{BODIPY}); \gamma(\text{N}_8, \text{B}, \text{C}_1, \text{C}_3);$ |
| 10 | b ₂ | 398(9.9) | def(m-ring); $\nu(\text{B}-\text{N}_{4a});$ | 432.2(27.1) | def(m-ring); $\nu(\text{B}-\text{N}_{4a});$ |
| 11 | a ₁ | 434.9(0.0) | breath(m-ring); $\delta(\text{m-ring}), \nu(\text{C}_8-\text{C}_{8a}), \nu(\text{B}-\text{N}_{4a}); \text{sci}(\text{F}-\text{B}-\text{F}); \nu(\text{C}_1-\text{C}_{8a});$ | 448.7(0.1) | breath(m-ring); $\delta(\text{m-ring}), \nu(\text{N}_8-\text{C}_{8a}), \nu(\text{B}-\text{N}_{4a}); \nu(\text{C}_1-\text{C}_{8a}); \text{sci}(\text{F}-\text{B}-\text{F});$ |
| 12 | b ₁ | 482.3(6.4) | $\gamma(\text{BF}_2); \gamma(\text{C}_8-\text{H});$ | 507.6(0.5) | $\gamma(\text{BF}_2); \gamma(\text{N}_8);$ |
| 13 | b ₁ | 596.4(18.9) | crown = $\gamma(\text{Py});$ | 584.7(16.3) | crown = $\gamma(\text{Py});$ |
| 14 | a ₁ | 598.3(4.9) | sci(F-B-F); $\nu(\text{B}-\text{F}); \nu(\text{B}-\text{N}_{4a}); \delta(\text{N}_{4a}-\text{B}-\text{N}_{4b});$ | 597.5(6.8) | sci(F-B-F); $\nu(\text{B}-\text{F}); \nu(\text{B}-\text{N}_{4a}); \delta(\text{N}_{4a}-\text{B}-\text{N}_{4b});$ |
| 15 | a ₂ | 607.5(0.0) | lightning = $\gamma(\text{Py});$ | 602.6(0.0) | lightning = $\gamma(\text{Py});$ |

* Based on PED. Coordinates are listed if their contributions are greater than ~10%. Coordinates are presented in descending order of their contributions. The designation “*Coord-1; Coord-2, Coord-3;*” means that the displacement along coordinates *Coord-2* and *Coord-3* are a part of the general displacement *Coord-1*. Given that the molecules have the symmetry C_{2v}, the following pairs of atoms are symmetrically equivalent: N_{4a} and N_{4b}, C₁ and C₇, C₂ and C₆, C₃ and C₅, C_{8a} and C_{8b}, H₁ and H₇, H₂ and H₆, H₃ and H₅, two fluorine atoms. Therefore, it is assumed in the assignment that, for example, vibration $\nu(\text{B}-\text{N}_{4a})$ includes both vibration $\nu(\text{B}-\text{N}_{4a})$ and $\nu(\text{B}-\text{N}_{4b})$, etc. The following designations are used: $\nu(\text{X}-\text{Y})$ – stretching of the X–Y bond; δ – in-plane bending of the fragment indicated in parentheses, including def – deformation of the fragment indicated in parentheses in the molecule plane; γ – out-of-plane bending of the fragment or atom indicated in parentheses; rot(fragment; axis) – rotation of the fragment around an axis; butterfly – butterfly-shape nonplanar molecular deformation; rot(BF₂) – rotation of the BF₂ fragment around an axis B–X₈; propeller – propeller-shape nonplanar molecular deformation; wag – wagging deformation in which two fluorine atoms oscillate up and below the plane BF₂ with respect to the boron atom; sci(F-B-F) – scissors bending of BF₂; fold(fragment; line) – folding of the fragment along the line; wav – wave-shape nonplanar molecule deformation, which can also be considered as chair-shaped folding of the molecule along the lines N_{4a}-C_{8a} and N_{4b}-C_{8b}; breath – breathing deformation of the fragment indicated in parentheses; crown – out-of-plane crown-shape bending of a molecule; lightning – lightning-shape out-of-plane bending of a molecule; m-ring – fragment B–N_{4a}-C_{8a}-X₈-C_{8b}-N_{4b}; Py – pyrrole moiety; Ct – center of internuclear distance. The designation “C–H Py” means C₁-H₁, C₂-H₂, C₃-H₃.

Table 3. Calculated frequencies (ω_i , cm^{-1}), IR-intensities ($I_{\text{IR}i}$, km mol^{-1}) and vibrational modes descriptions* for BODIPY and aza-BODIPY in the 650–1700 cm^{-1} range.

| i | sym | BODIPY | | Exp [13] | aza-BODIPY | |
|----|----------------|----------------------------|--|-------------|----------------------------|--|
| | | $\omega_i(I_{\text{IR}i})$ | Assignment* | | $\omega_i(I_{\text{IR}i})$ | Assignment* |
| 16 | a ₂ | 689.0(0.0) | $\gamma(\text{Py}); \gamma(\text{N}_{4a}, \text{C}_{8a});$ | | 685.1(0.0) | $\gamma(\text{Py}); \gamma(\text{N}_{4a}, \text{C}_{8a});$ |
| 17 | b ₂ | 706.7(36.4) | def(BODIPY); $\nu(\text{C}-\text{C}); \nu(\text{C}_8-\text{C}_{8a}); \nu(\text{B}-\text{N}_{4a});$ | 691 | 709.5(44.3) | def(BODIPY); $\nu(\text{B}-\text{N}_{4a});$ |
| 18 | b ₁ | 738.3(18.2) | $\gamma(\text{BODIPY}); \gamma(\text{N}_{4a}, \text{C}_{8a}, \text{C}_8); \gamma(\text{C}-\text{H}); \gamma(\text{C}_1-\text{H}_1);$ | | 750.0(33.4) | $\gamma(\text{BODIPY}); \gamma(\text{N}_{4a}, \text{C}_{8a}, \text{N}_8); \gamma(\text{C}-\text{H}); \gamma(\text{C}_1-\text{H}_1), \gamma(\text{C}_2-\text{H}_2);$ |
| 19 | a ₂ | 774.4(0.0) | $\gamma(\text{C}-\text{H}); \gamma(\text{C}_2-\text{H}_2), \gamma(\text{C}_1-\text{H}_1); \gamma(\text{BODIPY}); \gamma(\text{C}_{8a});$ | | 782.2(0.0) | $\gamma(\text{C}-\text{H}); \gamma(\text{C}_2-\text{H}_2), \gamma(\text{C}_1-\text{H}_1); \gamma(\text{BODIPY}); \gamma(\text{C}_{8a});$ |
| 20 | b ₁ | 776.0(84.6) | $\gamma(\text{C}-\text{H}); \gamma(\text{C}_2-\text{H}_2), \gamma(\text{C}_1-\text{H}_1); \gamma(\text{BODIPY}); \gamma(\text{C}_{8a});$ | 758 | 796.7(77.4) | $\gamma(\text{C}-\text{H}); \gamma(\text{C}_2-\text{H}_2), \gamma(\text{C}_1-\text{H}_1); \gamma(\text{BODIPY}); \gamma(\text{C}_{8a});$ |
| 21 | a ₁ | 814.5(6.0) | def(BODIPY); $\delta(\text{C}_{8a}-\text{C}_8-\text{C}_{8b}), \delta(\text{N}_{4a}-\text{C}_{8a}-\text{C}_8), \delta(\text{C}_{8a}-\text{C}_1-\text{C}_2); \nu(\text{N}-\text{C}); \delta(\text{C}-\text{H});$ | | 796.7(0.3) | def(BODIPY); $\delta(\text{C}_{8a}-\text{N}_8-\text{C}_{8b}), \delta(\text{N}_{4a}-\text{C}_{8a}-\text{N}_8), \delta(\text{C}_{8a}-\text{C}_1-\text{C}_2); \nu(\text{N}-\text{C}); \nu(\text{N}_8-\text{C}_{8a});$ |
| 22 | b ₂ | 860.8(9.4) | def(BODIPY); $\delta(\text{C}_{8a}-\text{C}_1-\text{C}_2), \delta(\text{C}_1-\text{C}_2-\text{C}_3); \nu(\text{B}-\text{N}_{4a}); \nu(\text{C}-\text{C});$ | | 857.3(1.8) | def(BODIPY); $\delta(\text{C}_1-\text{C}_2-\text{C}_3), \delta(\text{C}_{8a}-\text{C}_1-\text{C}_2); \nu(\text{B}-\text{N}_{4a});$ |

Assignment of the Vibrations of Unsubstituted BODIPY and Aza-BODIPY

Continuation of Table 3.

| | | | | | |
|----|----------------|----------------|--|--------------------|---|
| 23 | b ₁ | 873.7(7.1) | $\gamma(\text{C-H})$: $\gamma(\text{C}_3\text{-H}_3)$, $\gamma(\text{C}_1\text{-H}_1)$; $\gamma(\text{BODIPY})$; | 898.2(0.6) | $\gamma(\text{C-H})$: $\gamma(\text{C}_3\text{-H}_3)$, $\gamma(\text{C}_1\text{-H}_1)$; $\gamma(\text{BODIPY})$; |
| 24 | a ₂ | 880.3(0.0) | $\gamma(\text{C-H})$: $\gamma(\text{C}_3\text{-H}_3)$, $\gamma(\text{C}_1\text{-H}_1)$; $\gamma(\text{BODIPY})$; | 898.2(0.0) | $\gamma(\text{C-H})$: $\gamma(\text{C}_3\text{-H}_3)$, $\gamma(\text{C}_1\text{-H}_1)$; $\gamma(\text{BODIPY})$; |
| 25 | a ₁ | 909.2(1.1) | def(Py): $\delta(\text{C}_1\text{-C}_2\text{-C}_3)$, $\delta(\text{N}_{4a}\text{-C}_3\text{-C}_2)$; $\delta(\text{C-H Py})$; $\nu(\text{N}_{4a}\text{-C}_{8a})$; | 893.4(0.1) | def(Py): $\delta(\text{C}_1\text{-C}_2\text{-C}_3)$, $\delta(\text{N}_{4a}\text{-C}_3\text{-C}_2)$; $\delta(\text{C-H Py})$; $\nu(\text{N}_{4a}\text{-C}_{8a})$ |
| 26 | b ₂ | 920.0(7.9) | def(BODIPY); $\delta(\text{C-H})$; $\nu(\text{N}_{4a}\text{-C}_{8a})$; $\nu(\text{B-N}_{4a})$; | 910.6(8.2) | def(BODIPY); $\nu(\text{N}_{4a}\text{-C}_{8a})$; $\delta(\text{C-H})$; $\nu(\text{B-N}_{4a})$; |
| 27 | a ₂ | 922.2(0.0) | $\gamma(\text{C-H Py})$: $\gamma(\text{C}_3\text{-H}_3)$, $\gamma(\text{C}_2\text{-H}_2)$, $\gamma(\text{C}_1\text{-H}_1)$; fold(Py, C ₁ ...C ₃); | 933.0(0.0) | $\gamma(\text{C-H Py})$: $\gamma(\text{C}_2\text{-H}_2)$, $\gamma(\text{C}_3\text{-H}_3)$, $\gamma(\text{C}_1\text{-H}_1)$; fold(Py, C ₁ ...C ₃); |
| 28 | b ₁ | 922.4(2.0) | $\gamma(\text{C-H Py})$: $\gamma(\text{C}_3\text{-H}_3)$, $\gamma(\text{C}_2\text{-H}_2)$, $\gamma(\text{C}_1\text{-H}_1)$; fold(Py, C ₁ ...C ₃); | 933.3(2.1) | $\gamma(\text{C-H Py})$: $\gamma(\text{C}_2\text{-H}_2)$, $\gamma(\text{C}_3\text{-H}_3)$, $\gamma(\text{C}_1\text{-H}_1)$; fold(Py, C ₁ ...C ₃); |
| 29 | b ₁ | 952.5(9.5) | $\gamma(\text{C}_8\text{-H}_8)$; $\gamma(\text{C}_8)$; $\gamma(\text{C-H Py})$; | — | — |
| 30 | a ₁ | 1004.4(92.9) | $\nu(\text{B-F})$; $\delta(\text{C-H Py})$; def(BODIPY); | 969 999.0(84.3) | $\nu(\text{B-F})$; $\delta(\text{C-H Py})$; def(BODIPY); |
| 31 | b ₂ | 1040.2(1.4) | $\delta(\text{C-H})$: $\delta(\text{C}_2\text{-H}_2)$, $\delta(\text{C}_3\text{-H}_3)$; $\nu(\text{C-C})$; $\nu(\text{C}_2\text{-C}_3)$; | 1034.2(56.2) | $\delta(\text{C-H})$: $\delta(\text{C}_2\text{-H}_2)$, $\delta(\text{C}_3\text{-H}_3)$; $\nu(\text{C-C})$; $\nu(\text{C}_2\text{-C}_3)$, $\nu(\text{C}_1\text{-C}_2)$; |
| 32 | a ₁ | 1071.1(82.7) | $\delta(\text{C-H})$: $\delta(\text{C}_2\text{-H}_2)$, $\delta(\text{C}_1\text{-H}_1)$; $\nu(\text{B-F})$; $\nu(\text{C-C})$; | 1070.1(74.0) | $\delta(\text{C-H})$: $\delta(\text{C}_2\text{-H}_2)$, $\delta(\text{C}_1\text{-H}_1)$; $\nu(\text{B-F})$; $\nu(\text{C-C})$; |
| 33 | b ₂ | 1086.9(334.9) | $\delta(\text{C-H})$: $\delta(\text{C}_1\text{-H}_1)$; $\nu(\text{C-C})$: $\nu(\text{C}_1\text{-C}_2)$; | 1063 1087.2(558.7) | $\delta(\text{C-H})$: $\delta(\text{C}_1\text{-H}_1)$, $\delta(\text{C}_2\text{-H}_2)$; $\nu(\text{C-C})$; $\nu(\text{C}_1\text{-C}_2)$; $\nu(\text{N-C})$; $\nu(\text{B-N}_{4a})$; |
| 34 | a ₁ | 1098.7(46.3) | $\delta(\text{C-H})$: $\delta(\text{C}_1\text{-H}_1)$, $\delta(\text{C}_3\text{-H}_3)$; $\nu(\text{C-C})$; $\nu(\text{C}_2\text{-C}_3)$, $\nu(\text{C}_1\text{-C}_2)$; | 1088.6(49.6) | $\delta(\text{C-H})$: $\delta(\text{C}_1\text{-H}_1)$; $\nu(\text{C-C})$: $\nu(\text{C}_2\text{-C}_3)$, $\nu(\text{C}_1\text{-C}_2)$; |
| 35 | b ₂ | 1136.8(263.1) | $\nu(\text{C-C})$: $\nu(\text{C}_2\text{-C}_3)$, $\nu(\text{C}_1\text{-C}_{8a})$; $\nu(\text{B-N}_{4a})$; $\nu(\text{N-C})$; $\delta(\text{C}_3\text{-H}_3)$; | 1112 1110.2(250.0) | $\nu(\text{C-C})$: $\nu(\text{C}_2\text{-C}_3)$, $\nu(\text{C}_1\text{-C}_{8a})$; $\delta(\text{C-H})$; $\delta(\text{C}_1\text{-H}_1)$, $\delta(\text{C}_3\text{-H}_3)$; $\nu(\text{N-C})$; $\nu(\text{B-N}_{4a})$; |
| 36 | b ₁ | 1160.6(241.1) | $\nu(\text{B-F})$; | 1166 1169.3(244.3) | $\nu(\text{B-F})$; |
| 37 | a ₁ | 1168.0 (147.6) | $\nu(\text{B-N}_{4a})$; $\nu(\text{B-F})$; $\nu(\text{C-C})$: $\nu(\text{C}_2\text{-C}_3)$; | 1166.9(173.8) | $\nu(\text{B-N}_{4a})$; $\nu(\text{B-F})$; $\nu(\text{C-C})$: $\nu(\text{C}_2\text{-C}_3)$; |
| 38 | b ₂ | 1184.5(32.8) | $\delta(\text{C-H})$: $\delta(\text{C}_8\text{-H}_8)$, $\delta(\text{C}_2\text{-H}_2)$; $\nu(\text{B-N}_{4a})$; $\nu(\text{C-C})$; $\nu(\text{N-C})$: $\nu(\text{N}_{4a}\text{-C}_{8a})$; | 1230.3(22.6) | $\delta(\text{C-H})$: $\delta(\text{C}_3\text{-H}_3)$, $\delta(\text{C}_1\text{-H}_1)$, $\delta(\text{C}_2\text{-H}_2)$; $\nu(\text{N-C})$: $\nu(\text{N}_{4a}\text{-C}_{8a})$; |
| 39 | a ₁ | 1260.3(4.0) | $\delta(\text{C-H})$: $\delta(\text{C}_3\text{-H}_3)$, $\delta(\text{C}_1\text{-H}_1)$, $\delta(\text{C}_2\text{-H}_2)$; | 1261.9(12.2) | $\delta(\text{C-H})$: $\delta(\text{C}_3\text{-H}_3)$, $\delta(\text{C}_1\text{-H}_1)$, $\delta(\text{C}_2\text{-H}_2)$; |
| 40 | b ₂ | 1279.5(15.2) | $\nu(\text{N-C})$: $\nu(\text{N}_{4a}\text{-C}_3)$; $\delta(\text{C-H})$: $\delta(\text{C}_8\text{-H}_8)$, $\delta(\text{C}_3\text{-H}_3)$; $\nu(\text{C-C})$; | 1270.4(100.4) | $\nu(\text{N-C})$: $\nu(\text{N}_{4a}\text{-C}_3)$; $\nu(\text{C-C})$; $\delta(\text{C-H})$; |
| 41 | b ₂ | 1328.2(295.4) | $\delta(\text{C-H})$: $\delta(\text{C}_8\text{-H}_8)$, $\delta(\text{C}_3\text{-H}_3)$, $\delta(\text{C}_1\text{-H}_1)$; $\nu(\text{N-C})$: $\nu(\text{N}_{4a}\text{-C}_{8a})$, $\nu(\text{N}_{4a}\text{-C}_3)$; $\nu(\text{C-C})$; | 1292 — | — |
| 42 | a ₁ | 1357.1(0.6) | $\nu(\text{N-C})$: $\nu(\text{N}_{4a}\text{-C}_3)$, $\nu(\text{N}_{4a}\text{-C}_{8a})$; $\nu(\text{C-C})$; $\nu(\text{C}_1\text{-C}_2)$, $\nu(\text{C}_1\text{-C}_{8a})$; | 1324.2(8.5) | $\nu(\text{N-C})$: $\nu(\text{N}_{4a}\text{-C}_{8a})$, $\nu(\text{N}_{4a}\text{-C}_3)$; $\nu(\text{C}_1\text{-C}_{8a})$; |
| 43 | b ₂ | 1393.6(8.6) | $\nu(\text{C-C})$: $\nu(\text{C}_1\text{-C}_{8a})$, $\nu(\text{C}_1\text{-C}_2)$; $\delta(\text{C-H})$; $\delta(\text{C}_1\text{-H}_1)$; $\nu(\text{N-C})$: $\nu(\text{N}_{4a}\text{-C}_{8a})$; | 1391(238.6) | $\nu(\text{C-C})$: $\nu(\text{C}_1\text{-C}_{8a})$, $\nu(\text{C}_1\text{-C}_2)$; $\delta(\text{C-H})$; $\delta(\text{C}_3\text{-H}_3)$, $\delta(\text{C}_1\text{-H}_1)$; $\nu(\text{N-C})$; |
| 44 | a ₁ | 1396.9(0.6) | $\nu(\text{C-C})$: $\nu(\text{C}_{8a}\text{-C}_8)$, $\nu(\text{C}_1\text{-C}_2)$; $\nu(\text{N}_{4a}\text{-C}_{8a})$; $\delta(\text{C-H})$: $\delta(\text{C}_1\text{-H}_1)$; | 1387.7(0.3) | $\nu(\text{N-C})$: $\nu(\text{N}_8\text{-C}_{8a})$, $\delta(\text{C-H})$: $\delta(\text{C}_1\text{-H}_1)$; $\nu(\text{C-C})$: $\nu(\text{C}_1\text{-C}_2)$; |
| 45 | b ₂ | 1437.9(154.6) | $\delta(\text{C-H})$: $\delta(\text{C}_2\text{-H}_2)$; $\nu(\text{C-C})$: $\nu(\text{C}_2\text{-C}_3)$, $\nu(\text{C}_1\text{-C}_2)$; | 1397 1420.1(172) | $\delta(\text{C-H})$: $\delta(\text{C}_2\text{-H}_2)$, $\delta(\text{C}_1\text{-H}_1)$; $\nu(\text{C-C})$; $\nu(\text{C}_2\text{-C}_3)$; $\nu(\text{N-C})$; |
| 46 | a ₁ | 1451.3(120.2) | $\nu(\text{C-C})$: $\nu(\text{C}_2\text{-C}_3)$, $\nu(\text{C}_1\text{-C}_2)$; $\delta(\text{C-H})$; $\delta(\text{C}_2\text{-H}_2)$; | 1410 1455.4(145.2) | $\nu(\text{C-C})$: $\nu(\text{C}_1\text{-C}_2)$, $\nu(\text{C}_2\text{-C}_3)$; $\delta(\text{C-H})$; $\delta(\text{C}_2\text{-H}_2)$; |
| 47 | a ₁ | 1531.2(17.9) | $\nu(\text{N}_{4a}\text{-C}_3)$; $\nu(\text{C-C})$: $\nu(\text{C}_1\text{-C}_{8a})$, $\nu(\text{C}_8\text{-C}_{8a})$; $\delta(\text{C}_{2,3}\text{-H}_{2,3})$; | 1560.2(18.8) | $\nu(\text{N-C})$: $\nu(\text{N}_{4a}\text{-C}_3)$; $\delta(\text{C}_{2,3}\text{-H}_{2,3})$; $\nu(\text{C-C})$; $\nu(\text{C}_1\text{-C}_{8a})$; |
| 48 | b ₂ | 1536.6(6.1) | $\delta(\text{C-H})$: $\delta(\text{C}_3\text{-H}_3)$; $\nu(\text{C-C})$: $\nu(\text{C}_1\text{-C}_2)$; $\nu(\text{N-C})$: $\nu(\text{N}_{4a}\text{-C}_3)$; | 1539.3(3.7) | $\delta(\text{C-H})$: $\delta(\text{C}_3\text{-H}_3)$, $\delta(\text{C}_2\text{-H}_2)$; $\nu(\text{C}_1\text{-C}_2)$; $\nu(\text{N-C})$: $\nu(\text{N}_{4a}\text{-C}_3)$; |
| 49 | a ₁ | 1578.5(0.2) | $\nu(\text{C-C})$: $\nu(\text{C}_8\text{-C}_{8a})$, $\nu(\text{C}_1\text{-C}_{8a})$, $\nu(\text{C}_1\text{-C}_2)$; $\delta(\text{C}_{1,3}\text{-H}_{1,3})$; $\nu(\text{N-C})$; | 1577.3(4.4) | $\nu(\text{C-C})$: $\nu(\text{C}_1\text{-C}_{8a})$, $\nu(\text{C}_1\text{-C}_2)$; $\nu(\text{N-C})$: $\nu(\text{N}_8\text{-C}_{8a})$; $\delta(\text{C}_{1,3}\text{-H}_{1,3})$; |
| 50 | b ₂ | 1648.1(726.4) | $\nu(\text{C-C})$: $\nu(\text{C}_8\text{-C}_{8a})$, $\nu(\text{C}_1\text{-C}_{8a})$; $\delta(\text{C}_8\text{-H}_8)$; | 1605 1585.6(501.1) | $\nu(\text{N-C})$: $\nu(\text{N}_8\text{-C}_{8a})$, $\nu(\text{C}_3\text{-N}_{4a})$; $\nu(\text{C-C})$; |

* Based on PED. Coordinates are listed if their contributions are greater than ~10%. Coordinate with the largest contribution was placed in the first place. The designation "Coord-1: Coord-2, Coord-3;" means that the displacement along coordinates Coord-2 and Coord-3 are a part of the general displacement Coord-1. Given that the molecules have the symmetry C_{2v}, the following pairs of atoms are symmetrically equivalent: N_{4a} and N_{4b}, C₁ and C₇, C₂ and C₆, C₃ and C₅, C_{8a} and C_{8b}, H₁ and H₇, H₂ and H₆, H₃ and H₅, two fluorine atoms. Therefore, it is assumed in assignment that, for example, vibration $\nu(\text{B-N}_{4a})$ includes both vibration $\nu(\text{B-N}_{4a})$ and $\nu(\text{B-N}_{4b})$, etc. A description of the taken designations is given in a footnote to the Table 2.

Table 4. Calculated frequencies (ω_i , cm^{-1}), IR-intensities ($I_{\text{IR}i}$, km mol^{-1}) and vibrational modes descriptions* for BODIPY and aza-BODIPY in the 3180–3280 cm^{-1} range.

| i | sym | BODIPY | | aza-BODIPY | |
|----|-------|----------------------------|---|----------------------------|---|
| | | $\omega_i(I_{\text{IR}i})$ | Assignment* | $\omega_i(I_{\text{IR}i})$ | Assignment* |
| 51 | a_1 | 3196.2(1.2) | $\nu(\text{C}_8\text{-H}_8)$; | – | – |
| 52 | b_2 | 3234.0(0.5) | $\nu(\text{C-H Py})$: $\nu(\text{C}_1\text{-H}_1)$, $\nu(\text{C}_2\text{-H}_2)$, $\nu(\text{C}_3\text{-H}_3)$; | 3235.4(4.0) | $\nu(\text{C-H Py})$: $\nu(\text{C}_3\text{-H}_3)$, $\nu(\text{C}_2\text{-H}_2)$; |
| 53 | a_1 | 3234.1(1.9) | $\nu(\text{C-H Py})$: $\nu(\text{C}_1\text{-H}_1)$, $\nu(\text{C}_2\text{-H}_2)$, $\nu(\text{C}_3\text{-H}_3)$; | 3235.7(0.0) | $\nu(\text{C-H Py})$: $\nu(\text{C}_3\text{-H}_3)$, $\nu(\text{C}_2\text{-H}_2)$; |
| 54 | b_2 | 3242.0(4.0) | $\nu(\text{C-H Py})$: $\nu(\text{C}_3\text{-H}_3)$, $\nu(\text{C}_1\text{-H}_1)$; | 3248.1(0.0) | $\nu(\text{C-H Py})$: $\nu(\text{C}_1\text{-H}_1)$, $\nu(\text{C}_2\text{-H}_2)$, $\nu(\text{C}_3\text{-H}_3)$; |
| 55 | a_1 | 3242.4(0.6) | $\nu(\text{C-H Py})$: $\nu(\text{C}_3\text{-H}_3)$, $\nu(\text{C}_1\text{-H}_1)$; | 3248.4(0.0) | $\nu(\text{C-H Py})$: $\nu(\text{C}_1\text{-H}_1)$, $\nu(\text{C}_2\text{-H}_2)$, $\nu(\text{C}_3\text{-H}_3)$; |
| 56 | b_2 | 3257.5(2.8) | $\nu(\text{C-H Py})$: $\nu(\text{C}_2\text{-H}_2)$, $\nu(\text{C}_3\text{-H}_3)$, $\nu(\text{C}_1\text{-H}_1)$; | 3262.2(1.4) | $\nu(\text{C-H Py})$: $\nu(\text{C}_1\text{-H}_1)$, $\nu(\text{C}_2\text{-H}_2)$; |
| 57 | a_1 | 3257.5(0.2) | $\nu(\text{C-H Py})$: $\nu(\text{C}_2\text{-H}_2)$, $\nu(\text{C}_3\text{-H}_3)$, $\nu(\text{C}_1\text{-H}_1)$; | 3262.3(0.0) | $\nu(\text{C-H Py})$: $\nu(\text{C}_1\text{-H}_1)$, $\nu(\text{C}_2\text{-H}_2)$; |

* Based on PED. Coordinates are listed if their contributions are greater than ~10%. Coordinate with the largest contribution was placed in the first place. The designation “Coord-1; Coord-2; Coord-3;” means that the displacement along coordinates Coord-2 and Coord-3 are a part of the general displacement Coord-1. Given that the molecules have the symmetry C_{2v} , the following pairs of atoms are symmetrically equivalent: N_{4a} and N_{4b} , C_1 and C_7 , C_2 and C_6 , C_3 and C_5 , C_{8a} and C_{8b} , H_1 and H_7 , H_2 and H_6 , H_3 and H_5 , two fluorine atoms. Therefore, it is assumed in assignment that, for example, vibration $\nu(\text{B-N}_{4a})$ includes both vibration $\nu(\text{B-N}_{4a})$ and $\nu(\text{B-N}_{4b})$, etc. A description of the taken designations is given in a footnote to the Table 2.

of unsubstituted BODIPY and aza-BODIPY dyes, modeled and compared their IR spectra.

Acknowledgements. The study of molecular structure of BODIPY and the assignment of vibrational modes were supported by the grant of the President of the Russian Federation (project MK-5965.2021.1.3). The performing QC calculations for aza-BODIPY was supported by the Russian Science Foundation (grant No. 19-73-10107). Comparison of the obtained data for BODIPY and aza-BODIPY was conducted in accordance with the Project FZZW-2020-0007 supported by the Ministry of Science and Higher Education of Russian Federation. The study was carried out using the resources of the Center for Shared Use of Scientific Equipment of the ISUCT (with the support of the Ministry of Science and Higher Education of Russian Federation, grant No. 075-15-2021-671). We thank G.V. Girichev for his help in conducting the calculations using computing resources of the Department of Physics of Ivanovo State University of Chemistry and Technology.

Supplementary materials. The video file with visualization of all vibrations is available on the website <https://macroheterocycles.isuct.ru/en/mhc213973p>.

References

- Marzari N., Ferretti A., Wolverton C. *Nat. Mater.* **2021**, *20*, 736–749.
- Schellhammer K.S., Li T.-Y., Zeika O., Körner C., Leo K., Ortman F., Cuniberti G. *Chem. Mater.* **2017**, *29*, 5525–5536.
- Zlatic K., Ayouchia H.B. El, Anane H., Mihaljević B., Basarić N., Rohand T. *J. Photochem. Photobiol. A Chem.* **2020**, *388*, 112206.
- Loudet A., Burgess K. *Chem. Rev.* **2007**, *107*, 4891–4932.
- Kumar P.P.P., Yadav P., Shanavas A., Neelakandan P.P. *Mater. Chem. Front.* **2020**, *4*, 965–972.
- Vodyanova O.S., Kochergin B.A., Usoltsev S.D., Marfin Y.S., Romyantsev E.V., Aleksakhina E.L., Tomilova I.K. *J. Photochem. Photobiol. A Chem.* **2018**, *350*, 44–51.
- Pogonin A.E., Shagurin A.Y., Savenkova M.A., Telegin F.Y., Marfin Y.S., Vashurin A.S. *Molecules.* **2020**, *25*, 5361.
- Kitagawa T., Ozaki Y. Infrared and Raman Spectra of Metalloporphyrins. In: *Metal Complexes with Tetrapyrrole Ligands I* (Buchler J.W., Ed.), Berlin, Heidelberg: Springer Berlin Heidelberg, **1987**. pp. 71–114.
- Sliznev V.V., Pogonin A.E., Ischenko A.A., Girichev G.V. *Macroheterocycles* **2014**, *7*, 60–72.
- Furer V.L., Vandyukov A.E., Majoral J.P., Caminade A.M., Kovalenko V.I. *Vib. Spectrosc.* **2014**, *70*, 78–88.
- Jiang J., Bao M., Rintoul L., Arnold D.P. *Coord. Chem. Rev.* **2006**, *250*, 424–448.
- Lee Y., Das S., Malamakal R.M., Meloni S., Chenoweth D.M., Anna J.M. *J. Am. Chem. Soc.* **2017**, *139*, 14733–14742.
- Arroyo I.J., Hu R., Merino G., Tang B.Z., Peña-Cabrera E. *J. Org. Chem.* **2009**, *74*, 5719–5722.
- Tram K., Yan H., Jenkins H.A., Vassiliev S., Bruce D. *Dyes Pigment.* **2009**, *82*, 392–395.
- Schmitt A., Hinkeldey B., Wild M., Jung G. *J. Fluoresc.* **2009**, *19*, 755–758.
- Zhang X., Zhang Y., Jiang J. *Vib. Spectrosc.* **2003**, *33*, 153–161.
- Jamróz M.H. *Spectrochim. Acta Part A Mol. Biomol. Spectrosc.* **2013**, *114*, 220–230.
- Frisch M.J., Trucks G.W., Schlegel H.B., Scuseria G.E., Robb M.A., Cheeseman J.R., Montgomery J.A., Vreven J.T., Kudin K.N., Burant J.C., Millam J.M., Iyengar S.S., Tomasi J., Barone V., Mennucci B., Cossi M., Scalmani G., Rega N., Petersson G.A., Nakatsuji H., Hada M., Ehara M., Toyota K., Fukuda R., Hasegawa J., Ishida M., Nakajima T., Honda Y., Kitao O., Nakai H., Klene M., Li X., Knox J.E., Hratchian H.P., Cross J.B., Adamo C., Jaramillo J., Gomperts R., Stratmann R.E., Yazyev O., Austin A.J., Cammi R., Pomelli C., Ochterski J.W., Ayala P.Y., Morokuma K., Voth G.A., Salvador P., Dannenberg J.J., Zakrzewski V.G., Dapprich S., Daniels A.D., Strain M.C., Farkas Ö., Malick D.K., Rabuck A.D., Raghavachari K., Foresman J.B., Ortiz J. V, Cui Q., Baboul A.G., Clifford S., Cioslowski J., Stefanov B.B., Liu G., Liashenko A., Piskorz P., Komaromi I.,

- Martin R.L., Fox D.J., Keith T., Al-Laham M.A., Peng C.Y., Nanayakkara A., Challacombe M., Gill P.M.W., Johnson B., Chen W., Wong M.W., Gonzalez C., Pople J.A., **2003**, Gaussian 03, Revision B.03.
19. Dunning T.H. *J. Chem. Phys.* **1989**, *90*, 1007–1023.
20. Pritchard B.P., Altarawy D., Didier B., Gibson T.D., Windus T.L. *J. Chem. Inf. Model.* **2019**, *59*, 4814–4820.
21. Feller D. *J. Comput. Chem.* **1996**, *17*, 1571–1586.
22. Schuchardt K.L., Didier B.T., Elsethagen T., Sun L., Gurumoorthi V., Chase J., Li J., Windus T.L. *J. Chem. Inf. Model.* **2007**, *47*, 1045–1052.
23. Vishnevskiy Y.V., Zhabanov Y.A. *J. Phys. Conf. Ser.* **2015**, *633*, 012076.
24. Zhurko G.A., Chemcraft - graphical software for visualization of quantum chemistry computations. <https://www.chemcraftprog.com> (accessed September 21, 2021).
25. Teets T.S., Updegraff J.B., Esswein A.J., Gray T.G. *Inorg. Chem.* **2009**, *48*, 8134–8144.
26. Petrusenko I.K., Petrusenko K.B. *Spectrochim. Acta - Part A Mol. Biomol. Spectrosc.* **2015**, *138*, 623–627.
27. Zhang X.F., Zhu J. *J. Lumin.* **2019**, *205*, 148–157.
28. Groom C.R., Bruno I.J., Lightfoot M.P., Ward S.C. *Acta Crystallogr. Sect. B Struct. Sci. Cryst. Eng. Mater.* **2016**, *72*, 171–179.
29. Mulliken R.S. *J. Chem. Phys.* **1955**, *23*, 1997–2011.
30. Gómez-Zavaglia A., Fausto R. *J. Phys. Chem. A* **2004**, *108*, 6953–6967.
31. Precomputed vibrational scaling factors. *NIST Comput. Chem. Comp. Benchmark Database.* **2021**, <https://cccbdb.nist.gov/vibscalejust.asp> (accessed September 21, 2021)
32. Russell D., Johnson I. *NIST Stand. Ref. Database Number 101.* **2020**.
33. Shchupak E.E., Ivashin N.V., Sagun E.I. *Opt. Spectrosc.* **2013**, *115*, 37–47.
34. Wang Y.W., Descalzo A.B., Shen Z., You X.Z., Rurack K. *Chem. – A Eur. J.* **2010**, *16*, 2887–2903.

Received 09.11.2021

Accepted 27.11.2021